Title
PRODUCTION PROPERTIES AND DECAY MODES OF THE o MESON

Authors
Lindsey, James S.
Smith, Gerald A.

Publication Date
1966-01-31

UCRL-16526 Rev.

University of California

Ernest O. Lawrence Radiation Laboratory

PRODUCTION PROPERTIES AND DECAY MODES OF THE ϕ MESON

DISCLAIMER

Submitted to
Physical Review

UCRL-16526 Rev.

UNIVERSITY OF CALIFORNIA

Lawrence Radiation Laboratory
Berkeley, California

AEC Contract No. W-7405-eng-48

PRODUCTION PROPERTIES AND DECAY MODES OF THE ϕ MESON

James S. Lindsey and Gerald A. Smith

January 31, 1966

Production Properties and Decay Modes of the ϕ Meson*

James S. Lindsey and Gerald A. Smith

Department of Physics and Lawrence Radiation Laboratory
University of California, Berkeley, California

January 31, 1966

ABSTRACT

The reaction $K^-p \rightarrow \Lambda\phi$ has been studied in an exposure of the Lawrence Radiation Laboratory 72-in. bubble chamber to a separated beam of 2.1- to 2.7-BeV/c K^- mesons. The decay branching ratios for K^+K^-, $K_1^0K_2^0$, $\rho\pi$, $\eta\gamma$, $\rho\gamma$, and $\omega\gamma$ have been measured, and the ratio $\beta = [\Gamma(\phi \rightarrow K_1^0K_2^0)/\Gamma(\phi \rightarrow K^+K^-)]$ has been used as a test of the ϕ's spin. The quantum numbers assigned to the ϕ, $J^{PG} = 1^{--}$ and $I = 0$, have been confirmed.

Production processes were investigated using the correlation-matrix method of Berman and Oakes. The low-momentum (2.1-BeV/c beam momentum) data fit a model of K and K^* exchange, but the high-momentum (2.45 to 2.7 BeV/c) data are inconsistent with the model. Also, other final states involving $K\bar{K}$ pairs were investigated and their cross sections measured, but except for the production of the reaction $K^-p \rightarrow Y_1^*(1385)\phi$, no previously unreported effects were observed.

I. INTRODUCTION

The ϕ meson was discovered by Bertanza et al.[1] at Brookhaven National Laboratory (BNL) using a K^- beam at 2.24 BeV/c directed into the BNL 20-in. hydrogen bubble chamber. Shortly thereafter its quantum numbers were determined independently by groups at Brookhaven[2] and U. C. L. A.[3] In spite of its low cross section, the ϕ is easily seen in the final states $\Lambda K^+ K^-$ and $\Lambda K_1^0 K_2^0$, since the background in these channels is very small. The meson has been reported to have $J^{PG} = 1^{--}$ and isospin zero, exactly the same quantum numbers as those of the ω.

One puzzling aspect of the ϕ is its lack of decay into $\rho\pi$. Phase-space calculations indicate that this decay mode should dominate,[4] but this experiment and others have shown that it is suppressed by at least a factor of 3. Further, the ϕ is seldom seen in $\pi^- p$ reactions.[5]

Unitary Symmetry, or SU_3, has been remarkably successful in relating elementary particles as members of groups. In particular, the Gell-Mann–Okubo mass formula has been successfully applied to the pseudoscalar octet of mesons (π, K, η), the baryon octet (N, Λ, Σ, Ξ), and the baryon decuplet [$N^*(1238)$, $Y^*(1385)$, $\Xi^*(1530)$, Ω^-], but is far off when applied to an octet of vector mesons. From the masses of $K^*(888)$ and $\rho(750)$, the formula predicts a singlet at 930 MeV. The two known candidates, $\omega(782)$, and $\phi(1020)$, are too far from 930 MeV to be considered members of the octet.

A more recent theory of ω-ϕ mixing, due to Sakurai,[4] Glashow,[6] and others, accounts for the violation of the mass formula, accomodates suppression of the decay mode $\phi \rightarrow \rho\pi$, and in addition, predicts widths for ϕ decay into $\eta\gamma$ and $\pi^0\gamma$.

Production mechanisms in the reaction $K^-p \rightarrow \Lambda\phi$ have not been investigated in detail in previous experiments because of a lack of statistics. The exchange model has had considerable success in explaining processes such as $K^+p \rightarrow N^*K^*$, $\pi^+p \rightarrow N^*\rho$, etc.[7,8] in terms of pion exchange. The reaction $K^-p \rightarrow \Lambda\phi$ requires exchange of K or K^* mesons, and an investigation of this reaction as well as $K^-p \rightarrow \Lambda\omega$ might shed more light on the exchange process itself.

This experiment was undertaken to increase the statistics of K^-p reactions in the 2.1- to 2.7-BeV/c region of K^- momentum, and has provided several times as much data as any previous experiment done in this range. Several projects are therefore possible: (1) to confirm, with greater statistical accuracy the quantum numbers of the ϕ, (2) to determine branching ratios more accurately than before, and (3) to investigate ϕ-production mechanisms through final-state angular correlations.

II. EXPERIMENT

In the spring of 1963, the 72-in. hydrogen bubble chamber was exposed to a K^- beam constructed at the Bevatron.[9] The exposure lasted until early 1965, and consisted of 1,700,000 pictures. Of interest to this paper are 600,000 pictures in hydrogen at a beam momentum of 2.45 to 2.7 BeV/c, and 150,000 pictures at 2.1 BeV/c. At the highest

momentum setting the beam typically produced 6 to 7 K^- per pulse and an impurity of less than 20% π^-, with 1.5×10^{12} protons incident on an internal target and a full momentum bite ($\Delta p/p$) of 2%. Both flux and purity improved as the beam momentum was lowered.

Each roll of film was scanned once, and a large sample of film was second-scanned in order to provide information on scanning efficiencies for the various topologies of interest. These efficiencies were found to be typically 92 to 96%, depending on the topology and sample of film. Certain types of events were measured on Franckensteins and Scanning and Measuring Projectors (SMP's). Each event of interest was measured once, and samples of failing events (those events for which no passing hypothesis was found by the kinematics programs) were second- and third-measured to determine measuring efficiencies. The measurements were processed by the Alvarez group kinematics program, Package.[10]

III. THE REACTIONS $K^-p \to \Lambda K^+K^-$ AND $K^-p \to \Lambda K_1^0 K_2^0$; THE ϕ MESON

A. Ambiguities and Biases

From a total of 100,000 vee-two-prong events, approximately 450 gave an acceptable fit (confidence level greater than 0.005) to the hypothesis $K^-p \to \Lambda K^+K^-$. A Dalitz plot of events that fit the reaction is shown in Fig. 1(a). The dark band centered about a $K\bar{K}$ effective mass of 1020 MeV is a result of the reaction $K^-p \to \Lambda\phi$, $\phi \to K^+K^-$. The density of events in the ϕ band is much higher than that of the surrounding area, even though events that fit other hypotheses (for

example $K^- p \to \Lambda \pi^+ \pi^0 \pi^-$, $K^- p \to \Sigma^0 \pi^+ \pi^-$) have been included in the figure.[11] A study of these events has shown that the ϕ signal is as prominent in ambiguous events (many of which have even higher confidence levels for other hypotheses than for $K^- p \to \Lambda K^+ K^-$) as it is in unambiguous events. From this observation we conclude that substantially all events in Fig. 1(a) contain a $K^+ K^-$ pair, and the background produced by final states such as $\Lambda \pi^+ \pi^0 \pi^-$ and $\Sigma^0 \pi^+ \pi^-$ is negligible.

However, events of the type $K^- p \to \Sigma^0 K^+ K^-$, $\Sigma^0 \to \Lambda \gamma$ still may appear in Fig. 1(a), since this reaction is a copious source of ϕ's, also. We have therefore studied plots of the neutral mass (calculated using the measured momenta of the incident K^-, and outgoing K^+ and K^- tracks), and find that there is a very clean peak at the Λ mass with no apparent structure near the Σ^0 mass. From these considerations and the fact that the reaction $K^- p \to \Lambda K^+ K^-$ is fit with four constraints (since there are no invisible neutrals), we conclude that the ϕ region in Fig. 1(a) is, for our use, substantially free from contamination by other reactions.

The two-vee, zero-prong topology, of which 1700 events were found, contains events that fit the reaction $K^- p \to \Lambda K_1^0 K_2^0$. A Dalitz plot of these events is shown in Fig. 1(b). The ϕ ($K_1^0 K_2^0$ decay mode) is also quite prominent in this plot. We have compared ambiguous and unambiguous events fitting this reaction, and have come to the same conclusion that we reached above for $K^- p \to \Lambda K^+ K^-$--that these events are substantially free of contamination from reactions of the type $K^- p \to \Xi^0 K^0$, $\Lambda K_1^0 K_1^0$, $\Sigma^0 K_1^0 K_1^0$, etc. However, we may still have a substantial number

of events of the type $K^- p \to \Sigma^0 K_1^0 K_2^0$, $\Sigma^0 \to \Lambda\gamma$, since they would also contain a large percentage of ϕ's. This final state would appear among the (unfitted) $K^- p \to \Lambda K_1^0$ (+ neutrals) events. We have therefore plotted the missing neutral mass (effective mass of K_2^0 and γ in the $\Sigma^0 K_1^0 K_2^0$ case) and have found a large, symmetric peak about the K^0 mass (a signature of the $\Lambda K_1^0 K_2^0$ final state) with a tail of a few events extending upward in mass. This tail is probably the result of the Σ^0 reaction (since the $K_1^0\gamma$ effective mass must be greater than 518 MeV), and therefore these few events have been deleted from our sample of $K^- p \to \Lambda K_1^0 K_2^0$ events.

A search was also made for scanning or measuring losses that might affect angular distributions in these reactions. Several distributions (such as track length and angle of tracks with the camera axis) of the real events were compared with those of events obtained from the Monte-Carlo program Fake,[12] and the two sets of data were found to agree very closely (for both $\Lambda K^+ K^-$ and $\Lambda K_1^0 K_2^0$ final states). The only significant loss of events results from the decay of a Λ or K_1^0 very close (0.3 cm or less) to the primary vertex. These decay vertices are often confused with the primary vertex, itself. To correct for this loss, and also for the loss of events resulting from Λ and K_1^0 decays outside the chamber, we have used only events whose decay vertex (a) is 0.5 cm or more from the primary vertex, and (b) is inside a fiducial volume. We then weighted these decays with the inverse probability that (given their momentum, direction of motion, and point of origin) they will decay visibly (neither outside the decay fiducial

volume nor within 0.5 cm of the primary vertex). We believe that the application of all these considerations produces a sample of the reaction $K^- p \to \Lambda\phi$ which is essentially free from ambiguities and biases.

B. Production Processes

Figure 2 contains histograms of the square of the momentum transfer

$$\Delta^2_{p\to\Lambda} = (E_p - E_\Lambda)^2 - |\underset{\sim}{p}_p - \underset{\sim}{p}_\Lambda|^2 \qquad (1)$$

for $K^- p \to \Lambda\phi$ events. Both distributions show a definite peaking toward low values of Δ^2, and suggest that the production process may be dominated by K and K^* exchange, as shown in the inset of Fig. 2.

Berman and Oakes have suggested a method for studying reactions that produce resonant or unstable particles.[13] In particular, the method can be used to characterize the reaction $K^- p \to \Lambda\phi$, and to compare results with the theoretical predictions of K and K^* exchange. The basic idea is to write down all possible correlations between directions of decay products (proton from Λ decay, and K^+ or K_1^0 from ϕ decay) and the production directions K, L, and N (evaluated in the rest frame of the Λ or ϕ). All these directions are illustrated in Fig. 3.

As shown in Table I, there are six independent correlations for the ϕ and four for the Λ, so that the complete correlation matrix has 24 terms. Twelve of these are allowed by parity conservation and are indicated in Table I by $A_1 \ldots A_{12}$. The reaction is therefore characterized by an equation of the form

$$d\sigma = \sum_{i=1}^{12} A_i f_i, \qquad (2)$$

where:

$$f_1 = 1$$
$$f_2 = (\hat{e}\cdot\hat{K}_\phi)^2$$
$$f_3 = (\hat{e}\cdot\hat{N})^2$$
$$f_4 = (\hat{e}\cdot\hat{K}_\phi)(\hat{e}\cdot\hat{L}_\phi)$$
$$f_5 = (\hat{W}\cdot\hat{N})$$
$$f_6 = (\hat{W}\cdot\hat{N})(\hat{e}\cdot\hat{K}_\phi)^2$$
$$f_7 = (\hat{W}\cdot\hat{N})(\hat{e}\cdot\hat{N})^2$$
$$f_8 = (\hat{W}\cdot\hat{N})(\hat{e}\cdot\hat{K}_\phi)(\hat{e}\cdot\hat{L}_\phi)$$
$$f_9 = (\hat{W}\cdot\hat{K}_\Lambda)(\hat{e}\cdot\hat{K}_\phi)(\hat{e}\cdot\hat{N})$$
$$f_{10} = (\hat{W}\cdot\hat{K}_\Lambda)(\hat{e}\cdot\hat{L}_\phi)(\hat{e}\cdot\hat{N})$$
$$f_{11} = (\hat{W}\cdot\hat{L}_\Lambda)(\hat{e}\cdot\hat{K}_\phi)(\hat{e}\cdot\hat{N})$$
$$f_{12} = (\hat{W}\cdot\hat{L}_\Lambda)(\hat{e}\cdot\hat{L}_\phi)(\hat{e}\cdot\hat{N}).$$

Equation (2) is fit to the data by means of a maximum-likelihood fit. The probability of having event j in a certain configuration is

$$P_j = \sum_{i=1}^{12} A_i f_{ij}, \tag{3}$$

where f_{ij} denotes f_i evaluated for the jth event, and for normalization we set $A_1 + A_2/3 + A_3/3 = 1$.

The probability of having a group of events in a certain configuration is just the product:

$$P = \prod_j P_j. \tag{4}$$

The coefficients which give a best fit, then, are those for which P is a maximum. The method used to maximize P is to assume that it takes a gaussian form in A-space:

$$P = \exp\left[-1/2 \sum_{ij} (A_i - A_i^0)\, G_{ij} (A_j - A_j^0)\right] \qquad (5)$$

where A_i^0 are the values of A_i at the maximum, and G is a symmetric matrix independent of the A's. Then we can calculate

$$W = \log P = -1/2 \sum_{ij} (A_i - A_i^0)\, G_{ij} (A_j - A_j^0). \qquad (6)$$

Maximizing W is equivalent to maximizing P.

In interpreting the fit, it would be helpful to obtain an idea of the sensitivity of the value of P to changes in A_i. One can easily see that the form of W given above has a particularly simple second derivative:

$$\frac{\partial^2 W}{\partial A_i \partial A_j} = -G_{ij} . \qquad (7)$$

We can expand W in a Taylor series about its maximum point:

$$W - W_0 \approx \frac{1}{2} \sum_{ij} \frac{\partial^2 W}{\partial A_i \partial A_j}\Big|_0 \delta A_i \, \delta A_j .$$

Setting $W_0 - W = 1/2$ (equivalent to setting $P_0/P = \sqrt{e}$), we obtain a measure of how rapidly W varies with A_i:

$$\sum_{ij} G_{ij} \, \delta A_i \, \delta A_j = 1$$

and

$$\delta A_i \, \delta A_j = G_{ij}^{-1} , \qquad (8)$$

where G_{ij}^{-1} is the error matrix. The errors assigned to A_i in Tables II and III are the square roots of the diagonal terms:

$$\Delta A_i = \sqrt{G_{ii}^{-1}} . \qquad (9)$$

The data were divided up by incident momentum into two groups, the low-momentum group including the 2.1 BeV/c events, and the high-momentum group, which includes 2.45 through 2.7 BeV/c, since not enough events are available to make a further subdivision of the latter group meaningful. These groups are divided into three subgroups according to their momentum transfer squared, $\Delta^2_{p\to\Lambda}$. The results of fitting them, separately and together, are shown in Tables II and III.

One complication in the presentation of these tables is that the error under each term may not be correct, and may, in fact, be far too low. These are the correct errors only when the error matrix is diagonal, $G_{ij}^{-1} = 0$ for $i \neq j$. Otherwise, if there are large off-diagonal terms, A_i and A_j could be varied simultaneously in such a way as to decrease W by a relatively small amount. These off-diagonal terms decrease when the number of events is increased. For more than 100 events they become, on the average, less than 1/10 of the diagonal terms, but if less than 100 events are included in a fit, the quoted errors may be too low.

The only terms that consistently appear nonzero are A_1 and A_3. There is a slight hint that A_8 is also nonzero. Reference to Table I shows that A_1 and A_3 can come from K^* exchange, and that A_8 may arise from interference between K and K^* exchange. There appears to be no strong dependence upon Δ^2 in any of these terms, but the statistics are certainly not sufficient to make any study of Δ^2 dependence possible. At 2.1 BeV/c the data appear to be consistent with the exchange model, since (a) A_1, A_2, and A_3 have the correct signs and magnitudes, within errors, and (b) none of the "unallowed" terms

(A_4, A_5, A_6, A_7, A_{10}, and A_{12}) is nonzero. This conclusion is quite weak, since the large errors could be obscuring terms that are of considerable magnitude.

The high-momentum data, shown in Table III, presents an entirely different situation. The number of events in each category is much larger, and the production seems to be dominated by terms A_1, A_5, A_6, A_9, and A_{12}, most of which are not allowed by K and K^* exchange. In addition, the largest terms, A_9 and A_{12}, seem to increase in strength toward low values of Δ^2. It seems very improbable, therefore, that the reaction at this momentum can be explained by K and K^* exchange.

IV. THE ϕ MESON; OTHER DECAY MODES

In addition to the K^+K^- and $K_1^0K_2^0$ decay modes, the ϕ may have observable decay widths into other channels. In particular, the decay $\phi \to \rho\pi$ should have a considerable width. However, this experiment and others have shown that this mode is suppressed by at least a factor of 3 below phase-space predictions. The ω-ϕ mixing theory formulated by Sakurai[14] and Glashow[6] accomodates this anomaly and also explains the apparent failure of the Gell-Mann–Okubo mass formula as applied to the vector mesons.

Glashow has also shown that the matrix elements for the processes ϕ (or ω) $\to \pi\gamma$ or $\eta\gamma$ may be conveniently expressed in terms of the ω-ϕ mixing angle, θ ($\theta \approx 40$ deg from the $\phi\omega$ mass splitting) and the $\omega\rho\pi$ and $\phi\rho\pi$ coupling strengths. From the results of Barmin et al.[15] on the lower limit for $\omega \to \pi^0\gamma$ compared to $\omega \to \pi^+\pi^0\pi^-$, and the results

of Flatte et al,[16] on the value for $\omega \to$ (all neutrals) compared to $\omega \to \pi^+\pi^0\pi^-$, we have $\Gamma(\omega \to \pi^0\gamma) \approx 0.9$ MeV. Using this as input, and including a p^3 phase-space dependence, Glashow predicts

$$\Gamma(\omega \to \eta\gamma) \approx 0.002\,(1 - 5\epsilon)^2 \text{ MeV}, \tag{10a}$$

$$\Gamma(\phi \to \pi^0\gamma) \approx 2.1\,\epsilon^2 \text{ MeV}, \tag{10b}$$

and

$$\Gamma(\phi \to \eta\gamma) \approx 0.26\,(1 + 0.2\,\epsilon)^2 \text{ MeV}, \tag{10c}$$

where ϵ is the ratio of the $\phi\rho\pi$ to $\omega\rho\pi$ coupling strengths. Consequently, a value of ϵ is sufficient to complete the predictions.

If we assume $\epsilon \leq 0.2$ (the suppression of the decay $\phi \to \rho\pi$ would indicate that the $\phi\rho\pi$ coupling strength is small and therefore that ϵ is small), the equations above predict negligible widths for $\omega \to \eta\gamma$ and $\phi \to \pi^0\gamma$, but the width predicted for $\phi \to \eta\gamma$ is relatively independent of the value of ϵ. If we assume $\epsilon \approx 0$, we obtain $\Gamma(\phi \to \eta\gamma) = 0.26$ MeV, which might be experimentally visible.

A. $\rho\pi$ Decay Mode

The experiment has yielded a sample of 16,000 events which have a best fit to $\Lambda\pi^+\pi^0\pi^-$. Of these, a large fraction resulted from the intermediate state $Y_1^*(1385)\,\pi\pi$. The sample of events under investigation, therefore, includes only those which have no $\Lambda\pi$ combination with an effective mass between 1345 and 1425 MeV. In addition, we have selected only events that have low momentum transfer, $\Delta^2_{p\to\Lambda} \leq 0.8$ (BeV/c)^2 (since ϕ production is enhanced at low Δ^2), and events in which any $\pi\pi$ combination is in the ρ band (650 to 850 MeV).

A serious difficulty with this experiment results from the substantial ambiguity between $\Lambda\pi^+\pi^0\pi^-$, ΛK^+K^-, and other final states.

Of those events that pass as ΛK^+K^-, 65% also pass as $\Lambda 3\pi$. These events have been assigned to the ΛK^+K^- hypothesis and are no longer in the $\Lambda 3\pi$ sample; however, it may be possible that a ΛK^+K^- event which has been for some reason badly measured may not give an acceptable fit to ΛK^+K^-, but will still fit $\Lambda\pi^+\pi^0\pi^-$. The kinematics of this situation are such that the 3π effective mass of one fit will be very close to the K^+K^- mass of the other. Therefore, since the K^+K^- final state is dominated by ϕ production, a small number of these events ending up with a $\Lambda 3\pi$ assignment could produce a peak in the 3π effective mass spectrum in the ϕ region.

A true ΛK^+K^- event, even if badly measured, will have very little momentum unbalance. This effect will result in a very low momentum [in the laboratory (lab) system] being assigned to the π^0 in the $\Lambda 3\pi$ fit. A study of those events that passed both ΛK^+K^- and $\Lambda\pi^+\pi^0\pi^-$ hypotheses showed that the lab momentum of the π^0 was always less than 20 MeV, while the π^+ and π^- lab momenta were always much higher. In Fig. 4 we have plotted the lab momentum spectra for the π^0 (top) and the π^+ and π^- (bottom) for those events that (1) contain a $\pi\pi$ pair with effective mass in the ρ region, (2) contain no $\Lambda\pi$ pairs with effective mass in the Y^* band, (3) have $\Delta^2_{p\to\Lambda} \leq 0.8\ (\text{BeV/c})^2$, and (4) have a 3π effective mass in the ϕ region (1000 to 1040 MeV). Events that give an acceptable fit to ΛK^+K^- have been deleted from this sample.

The most striking feature of Fig. 4(a) is the large peaking near zero of the π^0 spectrum, while the $\pi^\pm$ spectrum of Fig. 4(b) appears more isotropic. This peaking can be due not only to ΛK^+K^- final states, but also to $\Lambda\pi^+\pi^-$, $\Sigma^0\pi^+\pi^-$, and $\Sigma^0K^+K^-$. In addition,

pion contamination in the beam can result in reactions such as $\pi^- p \to \Lambda K^+ \pi^-$ and $\pi^- p \to \Sigma^0 K^+ \pi^-$ which might produce the same effects. Due to the peripheral nature of these final states, the γ from Σ^0 decay is emitted preferably backward in the production c.m., resulting in a small lab momentum assignment for the π^0 in a fit to the event. The events in Fig. 4(a) that fit any of these reactions have been shaded, and it can be seen that they generally have π^0 lab momenta less than 50 MeV/c. It seems quite probable, then, that the peaking we observe in Fig. 4(a) is due to these other reactions being misidentified as $\Lambda 3\pi$.

A further requirement for our "clean" sample of $\Lambda 3\pi$ events, therefore, is that the π^0 lab momentum be greater than 50 MeV/c. The remaining data are plotted in two ways in Fig. 5. The top graph shows the "fitted" information, which assumes that the missing neutral is a π^0, while the bottom graph shows the "unfitted" or missing-mass information for the same events. The $\eta'(959)$ ($\pi^+\pi^-\gamma$ decay mode) appears in both histograms, but its mass has been pulled upward by the neutral assignment to a π^0 in the fitted data.

It is very difficult to draw a background curve for either histogram in Fig. 5 because of the presence of the $\eta'(959)$, and the extremely high level of ambiguity between $\Lambda 3\pi$ and $\Lambda\pi^+\pi^-\gamma$ hypotheses makes very difficult any attempt to separate the η' peak from the background under it. Referring to Fig. 5(a), there are 137 ± 12 events in the ϕ region (1000 to 1040 MeV), and our best estimate of the background is 107 ± 15 events (the error here is not statistical in nature, but reflects our ignorance of where to draw the phase-space curve). If we assume the back-

ground error to be Gaussian, the two errors can be folded together to obtain a ϕ signal of 30 ± 20 events. The histogram of Fig. 5(b) is consistent with this number. Having subtracted events from our sample due to the cut on $\Lambda\pi$ effective mass and π^0 momentum, we must multiply this number by a correction factor of 2.1. (This factor has been determined by Monte Carlo generation of 750 events of the type $K^- p \to \Lambda\phi$, $\phi \to \rho\pi$. These events were generated with the same production cosine distribution as seen in $K^- p \to \Lambda\phi$, $\phi \to K\bar{K}$ events, and with an isotropic ϕ decay distribution.) The corrected ϕ peak then contains 63 ± 42 events.

B. $\eta\gamma$ Decay Mode

The decay $\phi \to \eta\gamma$, if it exists, is much more difficult to observe. Even if we restrict the analysis to the decay mode $\eta \to \pi^+\pi^-\pi^0$, the two neutral particles in the final state (π^0 and γ) force us to look at unfitted or "missing mass" events, in particular those vee-two-prong events that have $MM \geq 2M_{\pi^0}$. One selection can be made, however, on the effective mass of the $\pi^+\pi^-$ pair. If the π pair originates from an η, its effective mass will be less than $M_\eta - M_{\pi^0} = 415$ MeV.

Figure 6 is a histogram of the ($\pi^+\pi^-$MM) effective mass spectrum from $\Lambda\pi^+\pi^-$ (+ neutrals) events. The histogram contains only events whose $\Delta^2_{p\to\Lambda}$ is less than 0.8 $(\text{BeV}/c)^2$, and those events which have $M_{\pi^+\pi^-} \leq 0.415$ MeV are shaded. The striking feature of the plot is the peaking at 960 MeV, which corresponds to $\eta'(959) \to \eta\pi^+\pi^-$, $\eta \to$ neutrals. Very little structure is seen in either distribution at the ϕ mass, so that we can attribute 0 ± 30 events to $\phi \to \pi^+\pi^-$ (+ neutrals)

and 0 ± 20 events to $\phi \to \eta\gamma$, $\eta \to \pi^+\pi^0\pi^-$. Since the η decay into $\pi^+\pi^0\pi^-$ represents 31% of its total decay rate, we should multiply this number by 3.1 to obtain a correct upper limit for $\phi \to \eta\gamma$.

C. C-Violating Decay Modes, $\phi \to \rho\gamma$ and $\phi \to \omega\gamma$

The result of a search for these decay modes has been published previously.[17] Similar techniques were used to search for $\phi \to \rho\gamma$ as those described above for $\phi \to \rho\pi$. The decay $\phi \to \omega\gamma$ results in a $\Lambda\pi^+\pi^-$ (+ neutrals) final state, and the upper limit for this mode is nearly the same as for $\phi \to \pi^+\pi^-$ (+ neutrals). We see no evidence for the existence of either decay mode.

D. Branching Ratios

Table IV summarizes the information from each decay mode. Each channel should be corrected for "invisible" events, e.g. $\phi \to K_1^0 K_2^0$, $K_1^0 \to \pi^0\pi^0$, for phase space in the decay $\phi \to \rho\pi$, and for scanning and measuring efficiencies peculiar to the topologies and fits involved.

E. Cross Sections

Table V gives cross sections for $K^-p \to \Lambda\phi$, and Fig. 7 is a plot of these values vs beam momentum. Results of other experiments on $K^-p \to \Lambda\phi$ have also been included in Fig. 7.

V. OTHER FINAL STATES INVOLVING $K\bar{K}$ PAIRS

A project of considerable interest, but not directly connected with the ϕ meson, concerns the survey of other final states containing $K\bar{K}$ pairs. Those reactions produced by this experiment are:

(a) $K^- p \rightarrow \Lambda K_1^0 K_1^0$ } both K_1^0 decays are seen with

(b) $\Sigma^0 K_1^0 K_1^0$ } or without visible Λ decay

(c) $\Sigma^0 K^+ K^-$

(d) $\Sigma^+ K^0 K^-$

(e) $\Sigma^- \bar{K}^0 K^+$

(f) $\Lambda K_1^0 K_1^0 \pi^0$

(g) $\Lambda K^+ K^- \pi^0$

(h) $\Lambda K^+ \bar{K}^0 \pi^-$

(i) $\Lambda K^0 K^- \pi^+$

Reactions (a), (b), (f), (h), and (i) are relatively free of ambiguity if we insist upon at least two decays being visible. Similarly, if we insist upon seeing the K^0 decay in reactions (d) and (e), contamination from other states is also negligible. In section IIIA, the ambiguity between $\Lambda K^+ K^-$ and $\Sigma^0 K^+ K^-$ was found to be resolvable, and if we use the same criteria (that is, reject any event that fits $\Lambda K^+ K^-$), the $\Lambda K^+ K^-$ background can be eliminated from reaction (c). Reaction (g) is more difficult, since it appears in the vee-two-prong topology and its fit has only one constraint. Of the 61 events that gave a best fit to this reaction, 37 are unambiguous, and the rest give additional fits to either $\Lambda K^+ \bar{K}^0 \pi^-$ or $\Lambda K^0 K^- \pi^+$, where only the Λ decays visibly.

A. $\Lambda K \bar{K}$ and $\Sigma K \bar{K}$ Final States

The histograms of $K_1^0 K_1^0$ effective mass from reactions (a) and (b) are shown in Fig. 8. Although the detection probability for these events is quite low (a 4/9 probability that both K^0's will decay via a charged mode, and a 3/4 probability that they will decay inside

the chamber), no structure is apparent in either histogram. In particular, the $K_1^0 K_1^0$ enhancement at threshold is not seen.[18,19]

Figure 9 shows histograms of $K\bar{K}$ masses from reactions (c), (d), and (e). The ϕ is quite evident in the $\Sigma^0 K^+ K^-$ reaction, but the charged $K\bar{K}$ systems show no particular structure.

B. Four-Body Final States

The entire experiment yielded only three examples of reaction (f), not enough to make any sort of study feasible. Reaction (g), however, shows one very interesting property. In Fig. 10 is shown a triangle plot, with $\Lambda\pi^0$ effective mass along the x-axis, and K^+K^- effective mass along the y-axis. There is a considerable grouping of events whose $\Lambda\pi^0$ effective masses are in the $Y^*(1385)$ band and whose K^+K^- masses lie in the ϕ region. It appears, therefore, that this final state is dominated by the reaction $K^- p \rightarrow Y^* \phi$. We found that the unambiguous events tend to cluster in the ϕ band, and the ambiguous events populate the plot more or less isotropically, so it seems probable that the ambiguous events come primarily from other reactions.

The effective masses of the charged $K\bar{K}$ pairs from reactions (h) and (i) are plotted in Fig. 11(a). As in the charged events, no particular structure is apparent. Another plot of interest is that of the neutral $K\bar{K}\pi$ effective mass from reactions (f), (h), and (i). This plot is shown in Fig. 11(b), and also shows no appreciable deviation from phase space.

Table VI summarizes cross-section information for these states.

VI. CONCLUSIONS

This experiment has confirmed the results of Connoly et al.[2] and Schlein et al.[3] for the quantum numbers of the ϕ. If we assume that the ϕ decays into $K\bar{K}$ via the strong interactions, the decay $\phi \to K_1^0 K_2^0$ defines C and P (and thus L) to be odd. Comparison of the three $\Sigma K\bar{K}$ final states shows I = 0 (and consequently that G is odd) since no $\phi^{\pm}$ is seen in the reactions $\Sigma^{\mp} K^{\pm} K^0$, and the triangle inequality,

$$(\sigma_{\Sigma^+\phi^-})^{1/2} + (\sigma_{\Sigma^-\phi^+})^{1/2} \geq 2(\sigma_{\Sigma^0\phi^0})^{1/2}$$

is violated by more than five standard deviations.[20]

The spin was determined by both London et al.[21] and Schlein et al.[3] who used the dependence of the widths for ϕ decay into K^+K^- and $K_1^0K_2^0$ on angular-momentum barriers and therefore on spin. The ratio

$$\beta = \frac{\Gamma(\phi \to K_1^0 K_2^0)}{\Gamma(\phi \to K^+K^-)}$$

should have the value 0.65 for spin 1 and 0.34 for spin 3 (the value for spin 1 changes slightly if different parameters are used in the model, but the spin-3 prediction is much more stable). Our value from Table IV is $\beta = 0.85 \pm 0.11$, which is within two standard deviations of the prediction for spin 1 and more than four standard deviations from spin 3. It appears, then, that the ϕ has spin 1.

Our measurement of the width for the decay $\phi \to \rho\pi$ is smaller than values obtained by other experiments.[21] However, the width we measure, $\Gamma(\phi \to \rho\pi) \approx 0.4$ MeV, when compared to the value

$\Gamma(\omega \to 3\pi) \approx 8.5$ MeV,[22] lends credence to the approximation used in Eqs. (10) that $\epsilon \approx 0$. Our experimental results for the decay $\phi \to \eta\gamma$ (branching ratio = $0 \pm 8\%$) agree with the prediction of Eq. (10c) (approximately 8%). However this just means that our experiment is not sensitive enough to confirm or deny the prediction. The determination of the $\eta\gamma$ branching ratio remains an important test of the mixing theory.

ACKNOWLEDGMENTS

The authors wish to acknowledge the efforts of the scanning and measuring staff, and of the bubble-chamber crews headed by Mr. Robert Watt. In particular, we thank Dr. Joseph J. Murray, under whose direction the K^- beam was designed and built, and Professor Luis Alvarez for his support and encouragement in this experiment. We also thank Professor George Trilling for valuable conversations concerning the background in our $\Lambda 3\pi$ sample.

FOOTNOTES AND REFERENCES

*Work done under the auspices of the U. S. Atomic Energy Commission.

1. L. Bertanza et al., Phys. Rev. Letters 9, 180 (1962).
2. P. Connoly et al., Phys. Rev. Letters 10, 371 (1963).
3. P. Schlein, W. E. Slater, L. T. Smith, D. H. Stork, and H. K. Ticho, Phys. Rev. Letters 10, 368 (1963).
4. J. J. Sakurai, Phys. Rev. Letters 9, 472 (1962).
5. Richard Hess, Lawrence Radiation Laboratory, private communication, 1965. The cross section for $\pi^- p \rightarrow n\phi$ is about 30 μb, just above threshold, but decreases to zero rapidly as beam momentum increases.
6. S. L. Glashow, Phys. Rev. Letters 11, 48 (1963); Symmetries of Strong Interactions, lecture given at Summer School, Varenna, Italy, 1964 (to be published).
7. J. D. Jackson and H. Pilkuhn, Nuovo Cimento 33, 906 (1964).
8. R. W. Huff, Phys. Rev. 133, B1078 (1964).
9. J. J. Murray, J. Button-Shafer, F. T. Shively, G. H. Trilling, J. A. Kadyk, A Rittenberg, D. M. Siegel, J. S. Lindsey, and D. W. Merrill, Lawrence Radiation Laboratory Report UCRL-11426, July 1964 (unpublished).
10. For a description of measuring devices and analysis programs, see A. Rosenfeld and W. E. Humphrey, Ann. Rev. Nucl. Sci. 13, 103 (1963).
11. We have investigated the other final states that are ambiguous with $\Lambda K^+ K^-$, and except for $\Sigma^0 K^+ K^-$, none contain any appreciable

ϕ signal or any other effect that would simulate the ϕ in a ΛK^+K^- interpretation.

12. Gerald A. Lynch, Lawrence Radiation Laboratory Report UCRL-10335, July 1962 (unpublished).

13. S. M. Berman and R. J. Oakes, Phys. Rev. 135, B1034 (1964).

14. J. J. Sakurai, Phys. Rev. 132, 434 (1963).

15. V. V. Barmin, A. G. Dolgolenki, Yu. S. Krestnikov, A. G. Meshkovskii, Yu. P. Nikitin, and V. A. Shebanov, JETP 18, 1289 (1964).

16. S. M. Flatté, D. O. Huwe, J. J. Murray, J. Button-Shafer, F. T. Solmitz, M. L. Stevenson, and C. Wohl, Phys. Rev. Letters 14, 1095 (1965).

17. J. S. Lindsey and G. A. Smith, Phys. Rev. Letters 15, 221 (1965).

18. A. R. Erwin et al., Phys. Rev. Letters 9, 34 (1962).

19. G. Alexander et al., Phys. Rev. Letters 9, 460 (1962).

20. This argument assumes that a charged ϕ would decay via $K\bar{K}$; we have also looked in the $\Sigma^{\pm}\pi^{\mp}\pi^+\pi^-$ channels and see no decay of the form $\phi^{\pm} \rightarrow \pi^{\pm}\pi^+\pi^-$.

21. G. W. London, R. R. Rau, N. P. Samios, S. S. Yamamoto, M. Goldberg, S. Lichtman, M. Primer, and J. Leitner, Brookhaven National Laboratory Report BNL-9542 (C-58), 1965 (to be published in Phys. Rev.), have found the branching fraction for $\phi \rightarrow \rho\pi$ to be $23 \pm 12\%$, and J. Badier et al., Phys. Letters 17, 337 (1965) give a value of $51 \pm 9\%$.

22. The best measurements of the total widths of the ϕ and ω are 3.1 ± 1.0 MeV and 9.5 ± 2.1 MeV, respectively. See N. Gelfand,

D. Miller, M. Nussbaum, J. Ratau, J. Schultz, J. Steinberger, T. H. Tan, L. Kirsch, and R. Plano, Phys. Rev. Letters 11, 438 (1963).

Table I. Correlation matrix for $K^- p \to \Lambda\phi$. Angular correlations present in the process $K^- p \to \Lambda\phi$ are indicated by $A_1 \ldots A_{12}$. Correlations excited by K exchange, K^* exchange, and their interference are indicated by (K), (K^*), and ($K + K^*$), respectively; A_1 through A_{12} correspond to the coefficients in Tables V and VI. This table was taken, in large part, from Ref. 13.

Λ Correlations	ϕ Correlations					
	1	$(\hat{e}\cdot\hat{K}_\phi)^2$	$(\hat{e}\cdot\hat{N})^2$	$(\hat{e}\cdot\hat{K}_\phi)(\hat{e}\cdot\hat{L}_\phi)$	$(\hat{e}\cdot\hat{K}_\phi)(\hat{e}\cdot\hat{N})$	$(\hat{e}\cdot\hat{L}_\phi)(\hat{e}\cdot\hat{N})$
1	A_1 (K^*)	A_2 (K), (K^*)	A_3 (K^*)	A_4		
$\hat{W}\cdot\hat{N}$	A_5	A_6	A_7	A_8 ($K + K^*$)		
$\hat{W}\cdot\hat{K}_\Lambda$					A_9 ($K + K^*$)	A_{10}
$\hat{W}\cdot\hat{L}_\Lambda$					A_{11} ($K + K^*$)	A_{12}

Table II. Density matrix for low-momentum (2.1-BeV/c) data.

Δ^2 (BeV/c)^2	A_1	A_2	A_3	A_4	A_5	A_6	A_7	A_8	A_9	A_{10}	A_{11}	A_{12}
$\Delta^2 \leq 0.4$	1.187	0.377	-0.937	-0.137	1.632	-2.587	-2.212	0.947	0.011	-1.173	-0.220	-1.077
38 events		± 0.912	± 0.643	± 0.655	± 0.972	± 1.369	± 1.329	± 1.379	± 0.867	± 1.324	± 1.245	± 0.883
$0.4 \leq \Delta^2 \leq 0.8$	1.386	0.150	-1.309	0.396	-0.343	1.308	0.333	0.267	0.629	0.574	-0.300	-0.166
61 events		± 0.587	± 0.447	± 0.579	± 0.644	± 0.913	± 0.765	± 1.093	± 1.006	± 0.901	± 0.825	± 0.975
$0.8 \leq \Delta^2$	1.176	-0.075	-0.452	-2.347	1.399	-0.696	-0.787	5.522	1.211	-0.630	-1.429	1.523
56 events		± 0.593	± 0.539	± 0.800	± 1.123	± 1.33	± 1.606	± 1.529	± 0.941	± 0.760	± 1.036	± 0.842
$\Delta^2 \leq 0.8$	1.305	0.129	-1.046	0.276	0.2686	0.027	0.414	0.608	0.172	0.025	0.114	-0.669
99 events		± 0.447	± 0.345	± 0.439	± 0.501	± 0.768	± 0.605	± 0.814	± 0.610	± 0.646	± 0.645	± 0.638
All Δ^2	1.258	0.114	-0.888	-0.356	0.243	0.130	-0.238	1.087	0.528	0.069	-0.359	0.340
155 events		± 0.341	± 0.283	± 0.339	± 0.411	± 0.617	± 0.531	± 0.623	± 0.455	± 0.466	± 0.506	± 0.516

Table III. Density matrix for high-momentum (2.45- to 2.70-BeV/c) data.

Δ^2 (BeV/c)^2	A_1	A_2	A_3	A_4	A_5	A_6	A_7	A_8	A_9	A_{10}	A_{11}	A_{12}
$\Delta^2 \leq 0.4$	0.995	0.064	-0.048	0.013	-0.241	0.707	-0.429	-0.398	2.208	-0.019	0.043	2.996
144 events		±0.311	±0.312	±0.304	±0.266	±0.456	±0.507	±0.474	±0.404	±0.505	±0.604	±0.699
$0.4 \leq \Delta^2 \leq 0.8$	1.081	0.248	-0.490	0.089	-0.663	1.065	0.386	0.140	1.364	-0.2003	0.492	0.668
159 events		±0.316	±0.289	±0.322	±0.309	±0.509	±0.421	±0.557	±0.456	±0.530	±0.488	±0.471
$0.8 \leq \Delta^2$	1.255	-0.522	-0.242	-0.182	-0.431	0.598	0.420	0.444	0.552	-0.845	-0.613	0.962
106 events		±0.348	±0.389	±0.403	±0.436	±0.553	±0.720	±0.657	±0.625	±0.661	±0.657	±0.666
$\Delta^2 \leq 0.8$	1.011	0.187	-0.220	0.053	-0.480	0.937	0.150	-0.112	1.753	-0.017	0.197	1.306
303 events		±0.220	±0.216	±0.227	±0.215	±0.345	±0.341	±0.376	±0.308	±0.346	±0.363	±0.354
All Δ^2	1.097	-0.018	-0.273	0.236	-0.476	0.874	0.147	-0.038	1.435	-0.222	0.007	1.250
409 events		±0.188	±0.188	±0.196	±0.198	±0.295	±0.313	±0.325	±0.286	±0.297	±0.326	±0.311

UCRL-16526 Rev.

Table IV. Summary of ϕ decay modes.

ϕ decay mode	Number of observed events	Corrections		Corrected number of events	Branching ratio
		Invisible decays	Scan. and meas.		
K^+K^-	252 ± 16	1.0	1.4 ± .05	353 ± 26	48 ± 4
$K_1^0K_2^0$	167 ± 13	1.5	1.2 ± .09	301 ± 33	40 ± 4
$\rho\pi$	30 ± 20[a]	2.1[b]	1.4 ± .05	88 ± 59	12 ± 8
$\eta\gamma$	0 ± 14	3.1[c]	1.4 ± .05	0 ± 61	0 ± 8
$\pi^+\pi^-$ (+ neutrals)	0 ± 30	1.0	1.4 ± .05	0 ± 42	0 ± 5
$\rho\gamma$	0 ± 10	1.0	1.4 ± .05	0 ± 14	0 ± 2
$\omega\gamma$	0 ± 30	1.0	1.4 ± .05	0 ± 42	0 ± 5

[a] This error represents our estimated systematic error in calculating phase space, folded in with the statistical error.

[b] This correction replaces events deleted by ρ selections, Y^* cuts, etc.

[c] This factor corrects for η decays into "all neutral" modes not observed in this experiment.

Table V. Path lengths and cross sections for $K^- p \rightarrow \Lambda\phi$ and $\phi \rightarrow K\bar{K}$, $\rho\pi$.

Measured beam momentum (BeV/c)	Path length (events/μb)	Cross section[a] (μb)
2.10	5.20 ± .26	82 ± 11
2.43	1.78 ± .09	63 ± 11
2.58	3.43 ± .17	87 ± 12
2.61	5.96 ± .30	69 ± 9
2.68	3.07 ± .15	77 ± 11

[a]The cross sections have been corrected for scanning and measuring efficiencies and invisible Λ and K^0 decays.

Table VI. Cross sections for production of various final states.

Reaction	Cross section at 2.1 BeV/c[a] (μb)	Cross section at 2.45 to 2.7 BeV/c[a] (μb)
$K^- p \rightarrow \Lambda\phi$	82 ± 11	74 ± 8
$\rightarrow \Sigma^0\phi$	8 ± 3	20 ± 4
$\rightarrow Y^*(1385)\phi$	0	7.5 ± 3
$\rightarrow \Lambda K^+K^-$(non-$\phi$)	20 ± 4	43 ± 6
$\rightarrow \Lambda K^0\bar{K}^0$(non-$\phi$)	26 ± 6	80 ± 12
$\rightarrow \Sigma^0 K^+K^-$(non-$\phi$)	2 ± 2	10 ± 3
$\rightarrow \Sigma^+ K^0 K^-$	---	2 ± 1
$\rightarrow \Sigma^- K^+ \bar{K}^0$	---	7 ± 3
$\rightarrow \Lambda K^\pm K^0 \pi^\mp$	0	3 ± 1.5

[a]These cross sections have been corrected for scanning and measuring efficiencies and neutral decay modes.

FIGURE LEGENDS

Fig. 1. Dalitz plots for the reactions (a) $K^- p \to \Lambda K^+ K^-$ and (b) $K^- p \to \Lambda K_1^0 K_2^0$. Envelopes are for 2.1- and 2.7-BeV/c incident K^- momentum.

Fig. 2. Histogram of $\Delta^2_{p\to\Lambda}$ for $K^- p \to \Lambda K^+ K^-$ and $K^- p \to \Lambda K_1^0 K_2^0$ events whose $K\bar{K}$ effective mass is in the ϕ band (1000 to 1040 MeV). (a) Low-momentum (2.1 BeV/c) and (b) high-momentum (2.45 to 2.70 BeV/c) data. The inset shows a schematic diagram of the K and K^* exchange process.

Fig. 3. Coordinate system for $K^- p \to \Lambda\phi$ and the subsequent decays $\Lambda \to p\pi^-$, $\phi \to K\bar{K}$. All vectors have unit length. $\hat{K}_{c.m.}$ is the incoming beam direction in overall c.m., $\hat{\Lambda}_{c.m.}$ is the Λ direction in overall c.m., $\hat{\phi}_{c.m.}$ is the ϕ direction in overall c.m., $\hat{N}$ is the production normal, $\hat{K}_{c.m.} \times \hat{\Lambda}_{c.m.}$, and is in the same direction in all three frames, $\hat{L}_{c.m.}$ is $\hat{K}_{c.m.} \times \hat{N}$, $\hat{K}_\Lambda$, $\hat{K}_\phi$ is the incoming beam direction in Λ and ϕ c.m. systems, respectively, $\hat{L}_\Lambda$ is $\hat{K}_\Lambda \times \hat{N}$, $\hat{L}_\phi$ is $\hat{K}_\phi \times \hat{N}$, $\hat{W}$ is the decay proton direction in Λ c.m. frame, $\hat{e}$ is the decay K^+ or K_1^0 direction in ϕ c.m. frame.

Fig. 4. (a) Histogram of π^0 lab momentum for events whose best hypothesis is $K^- p \to \Lambda\pi^+\pi^0\pi^-$ and which have (1) no $\Lambda\pi$ combination whose effective mass is in the Y^*(1345- to 1425-MeV) band, (2) a $\pi\pi$ combination whose effective mass is in the ρ(650- to 850-MeV) band, (3) $\Delta^2_{p\to\Lambda} \leq 0.8\ (\text{BeV}/c)^2$, (4) no fit to $\Lambda K^+ K^-$, (5) a $\pi^+\pi^0\pi^-$ effective mass of 1000 to 1040 MeV. (b) Histogram

of π^+ and π^- lab momenta for the same events.

Fig. 5. Histograms of $\pi^+\pi^0\pi^-$ effective mass for $\Lambda 3\pi$ events that pass criteria (1), (2), (3), and (4) of Fig. 4 and whose π^0 lab momentum is less than 50 MeV/c. (a) Fitted information, assuming the missing neutral is a π^0. (b) Unfitted ($\pi^+\pi^-$MM) effective mass for the same events.

Fig. 6. Histogram of ($\pi^+\pi^-$MM) effective mass from $K^-p \to \Lambda\pi^+\pi^-$ (+ neutrals $\geq 2\pi^0$) events which have $\Delta^2_{p\to\Lambda} \leq 0.8\ (\text{BeV/c})^2$. The shaded events have $M_{\pi^+\pi^-} \leq 0.415$ BeV.

Fig. 7. Plot of total $K^-p \to \Lambda\phi$ cross section, corrected for all neutral decay modes.

Fig. 8. Histogram of $K_1^0K_1^0$ effective mass from (a) $\Lambda K_1^0K_1^0$ events and (b) $\Sigma^0K_1^0K_1^0$ events.

Fig. 9. Histograms of $K\bar{K}$ effective mass for the reactions (a) $\Sigma^0K^+K^-$, (b) $\Sigma^+K^0K^-$, and (c) $\Sigma^-K^+\bar{K}^0$.

Fig. 10. Scatter plot of $\Lambda\pi^0$ effective mass vs K^+K^- effective mass for $K^-p \to \Lambda K^+K^-\pi^0$ events.

Fig. 11. (a) Histogram of charged $K\bar{K}$ effective mass for $K^-p \to \Lambda K^+\bar{K}^0\pi^-$ and $\Lambda K^0K^-\pi^+$ events. (b) Histogram of neutral $K\bar{K}\pi$ effective mass for $\Lambda K^+\bar{K}^0\pi^-$, $\Lambda K^0K^-\pi^+$, and $\Lambda K_1^0K_1^0\pi^0$ events.

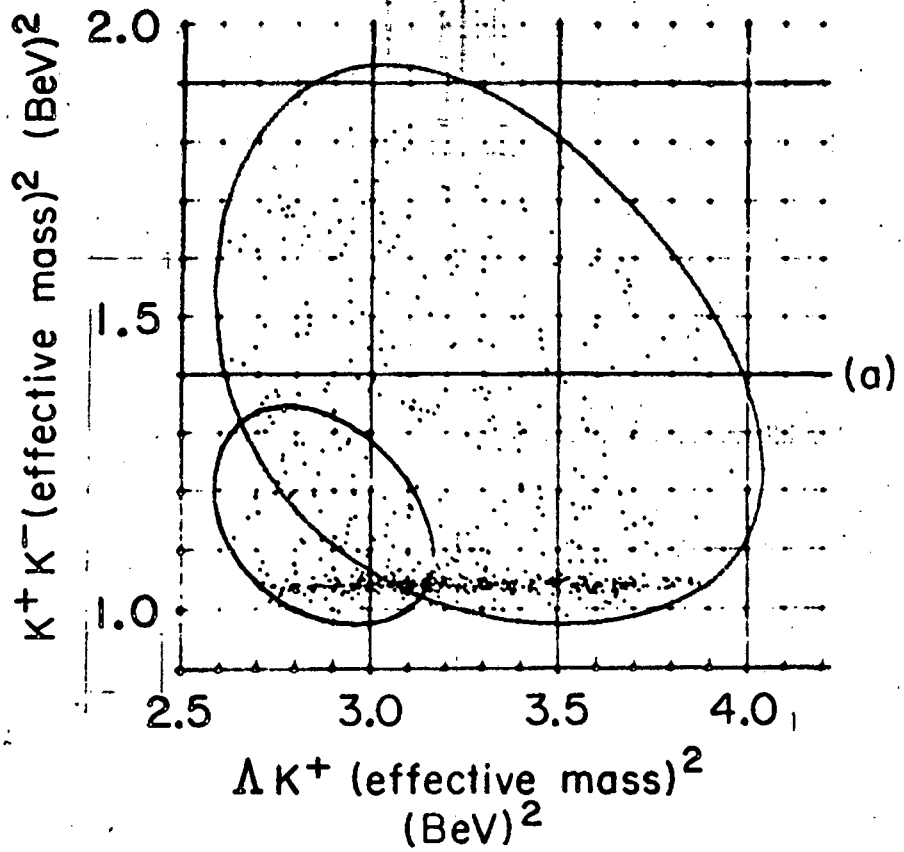

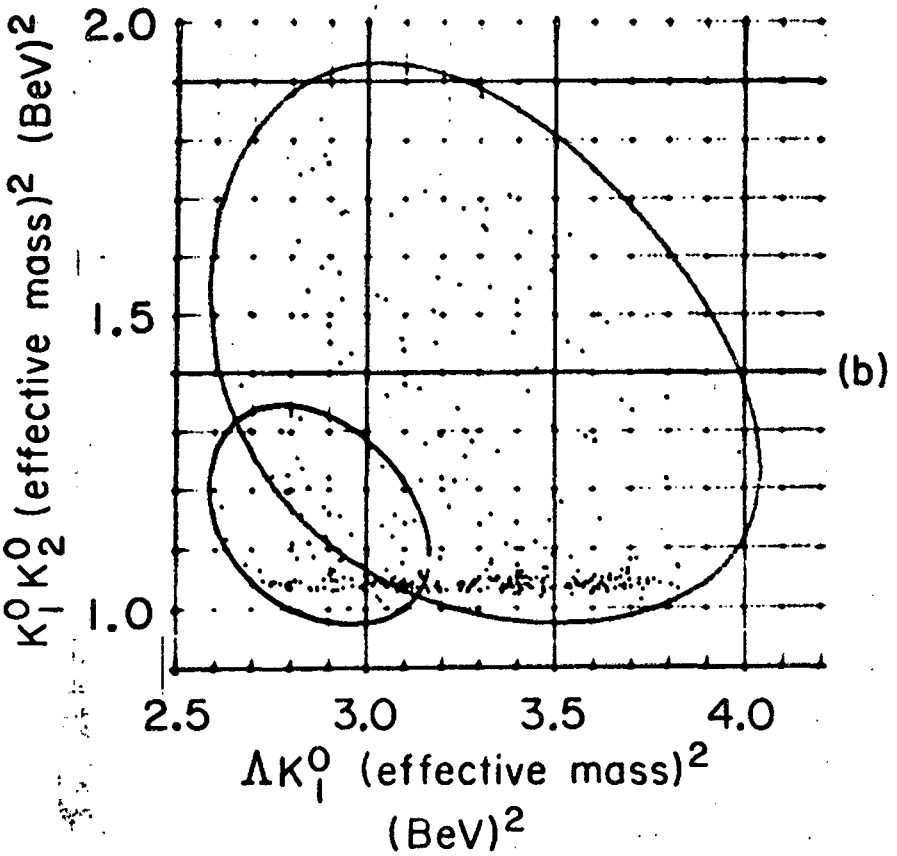

Fig. 1

MU-37102

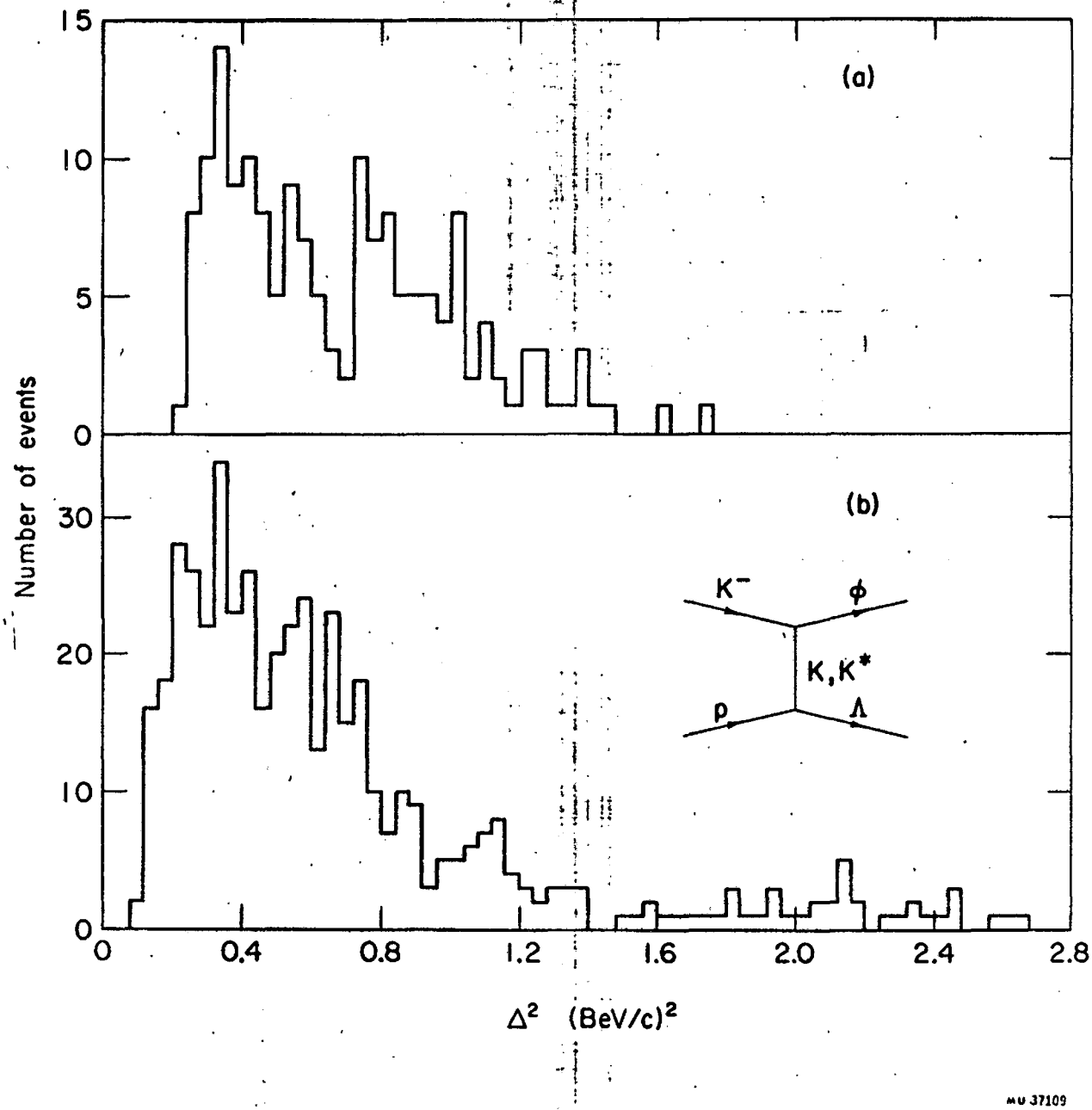
(a)
(b)
Number of events
15
10
5
0
30
20
10
0
0
0.4
0.8
1.2
1.6
2.0
2.4
2.8
Δ² (BeV/c)²
K⁻
φ
K, K*
p
Λ
MU 37109

Fig. 2

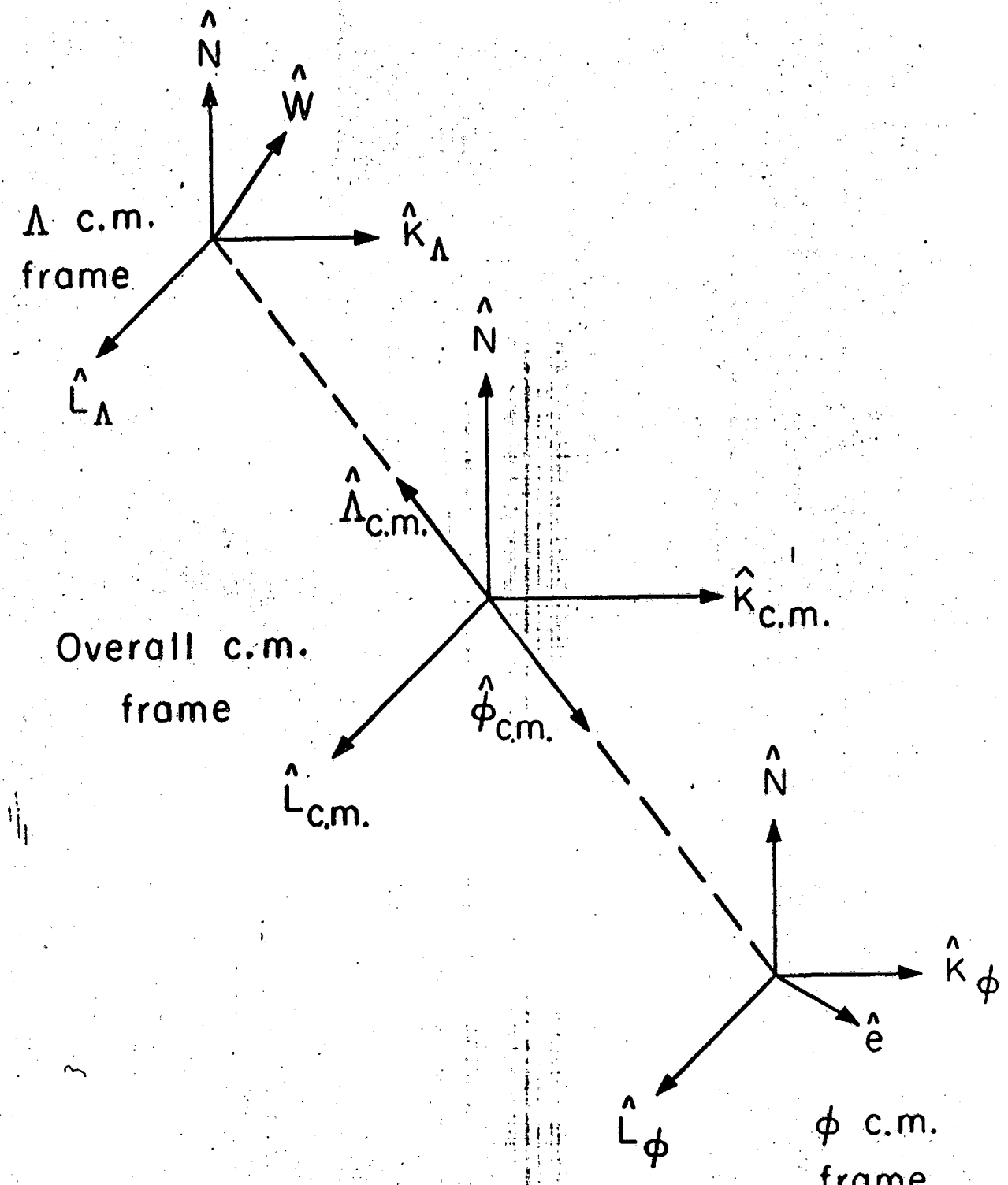

Fig. 3

MU-37098

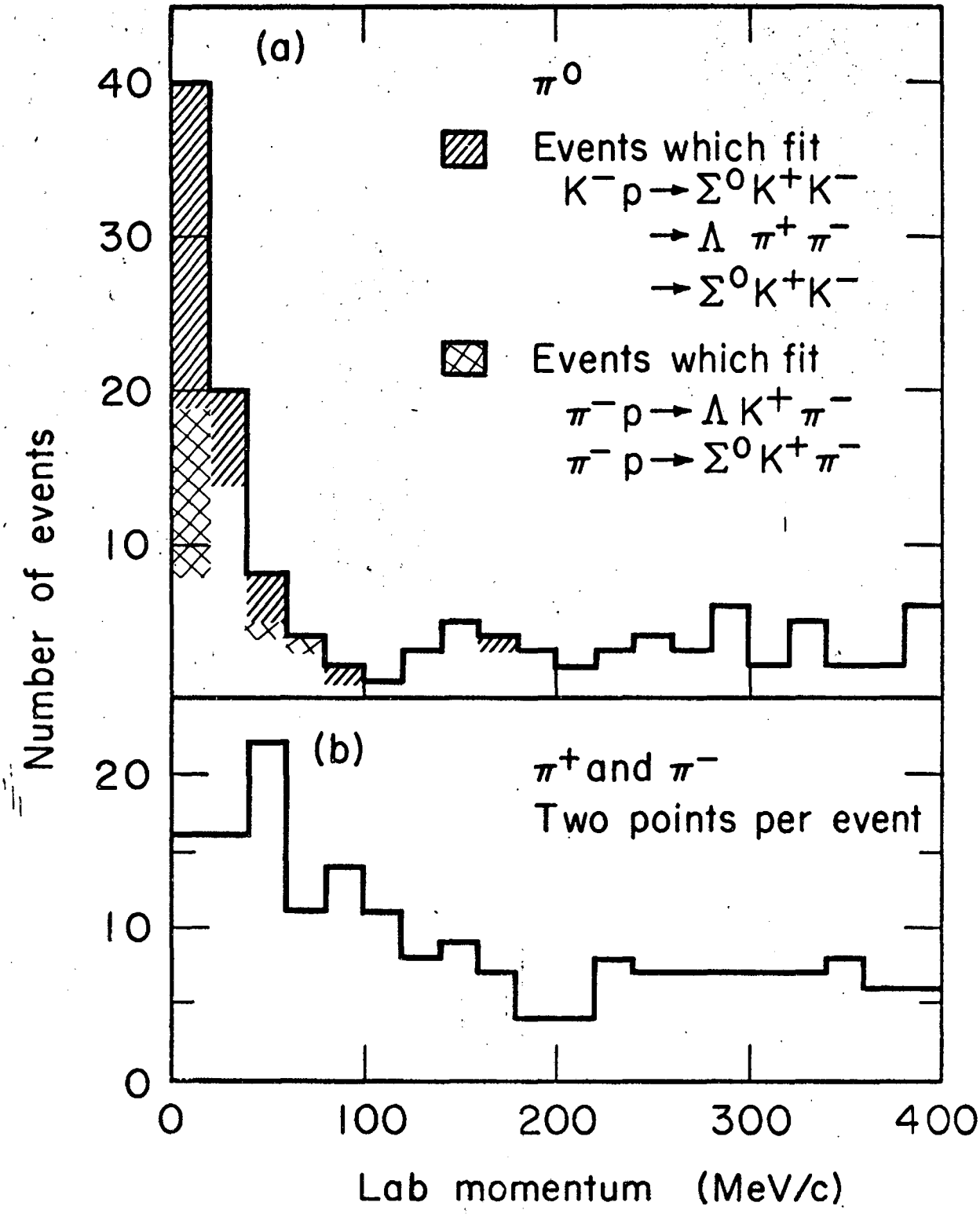

Fig. 4

MU-37110

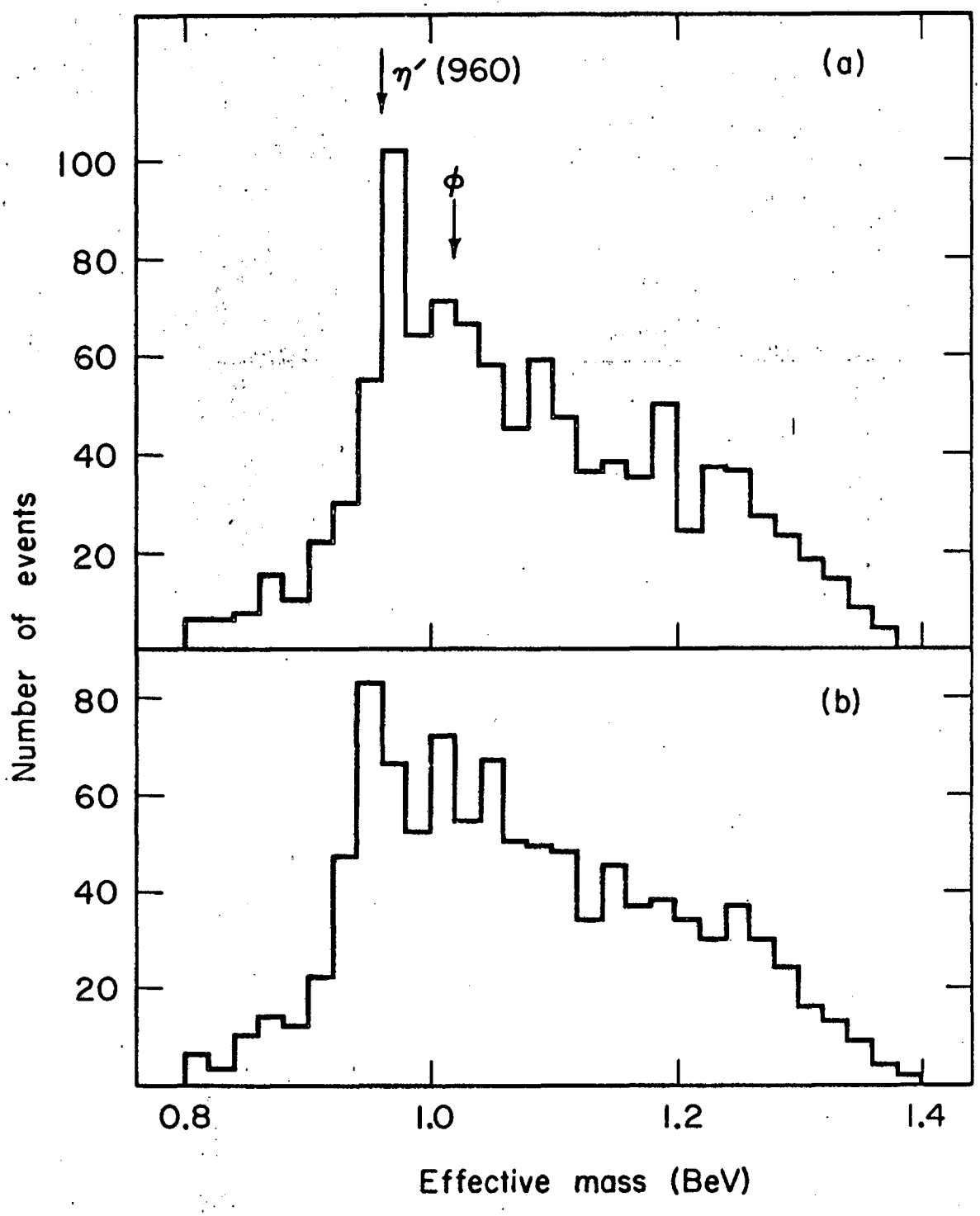
η′ (960)
(a)
φ
100
80
60
40
20
Number of events
(b)
80
60
40
20
0.8
1.0
1.2
1.4
Effective mass (BeV)
MU-37111

Fig. 5

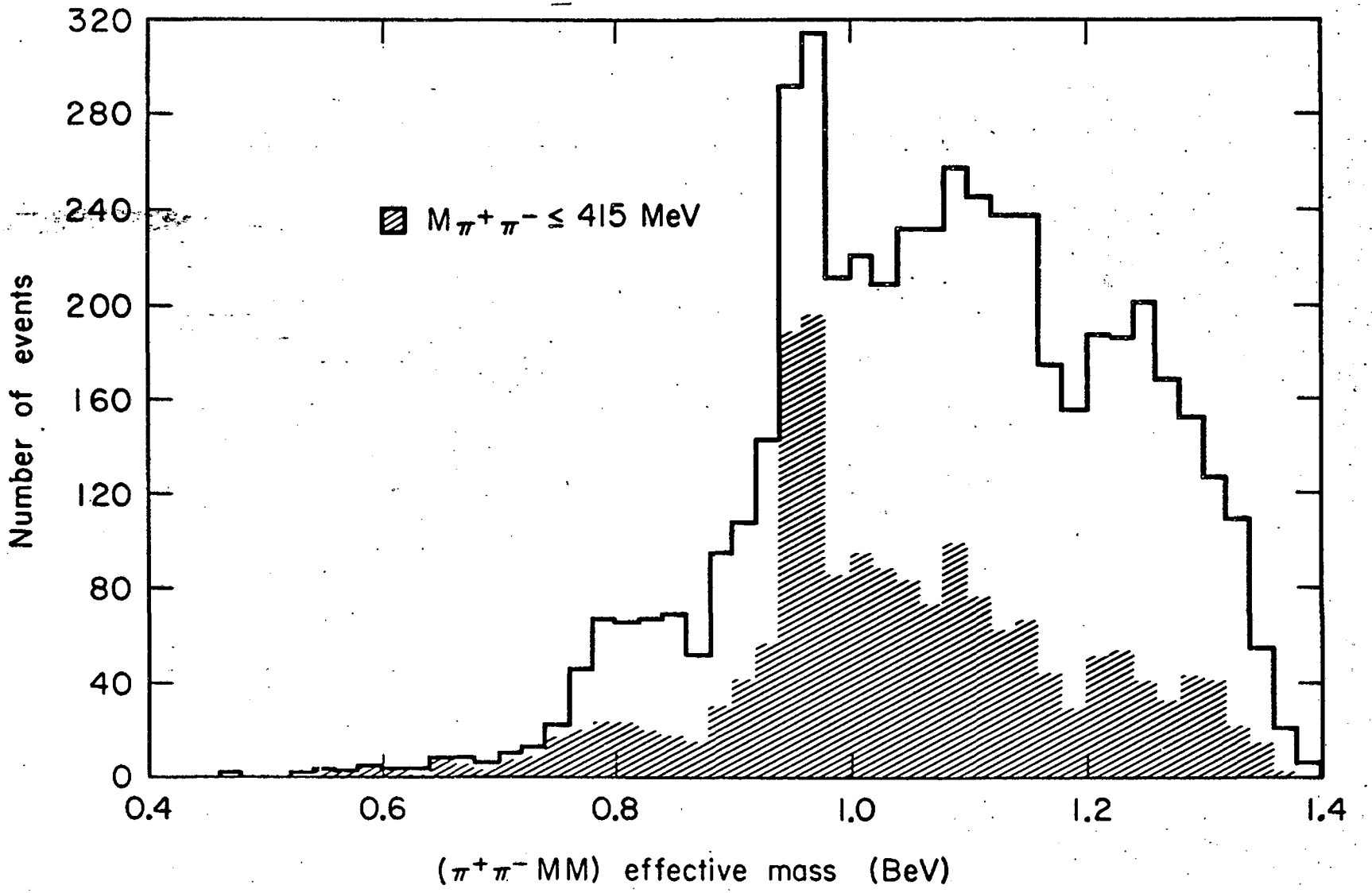

Fig. 6

MU-37112

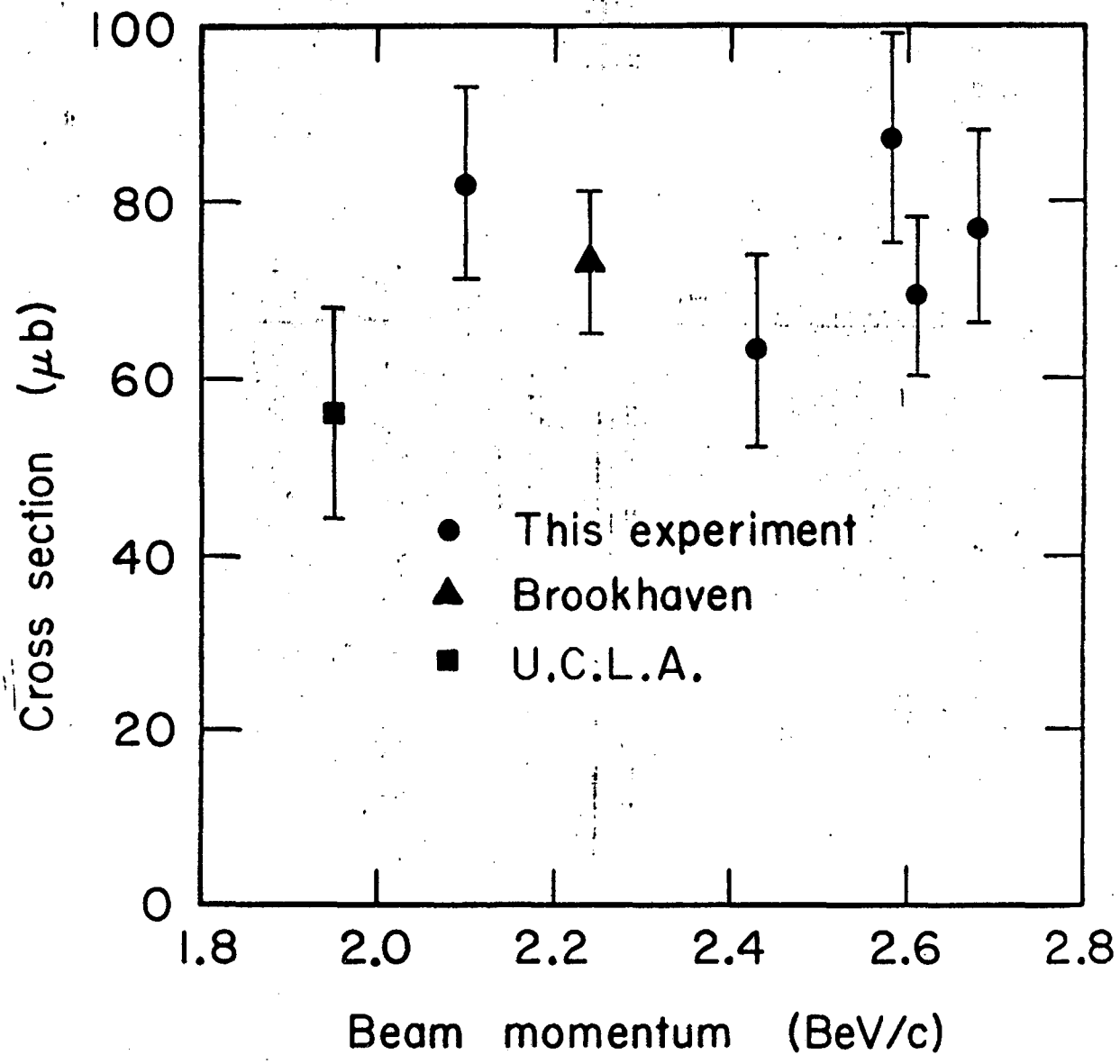

Fig. 7

MU-37114

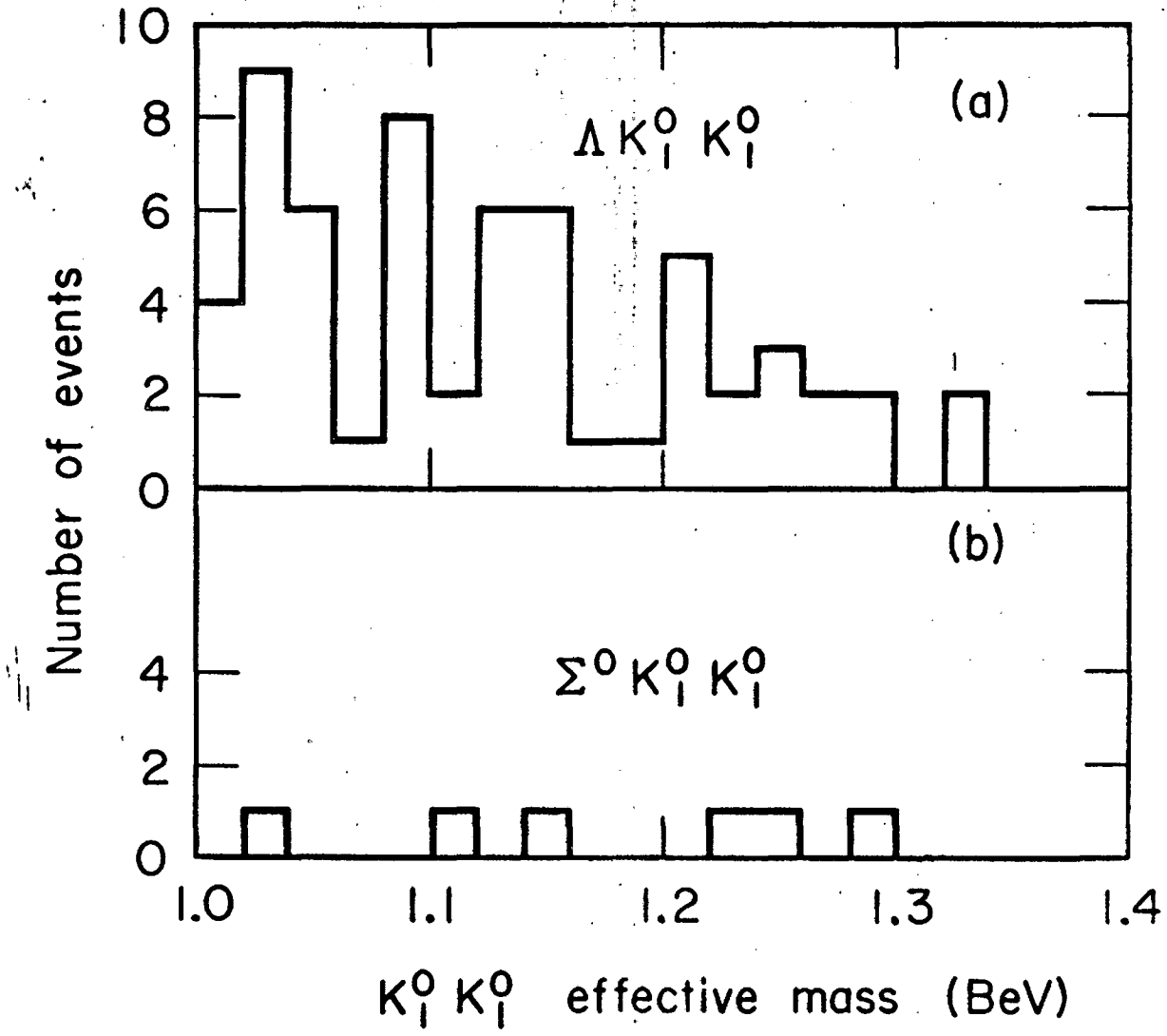

Fig. 8

MU-37115

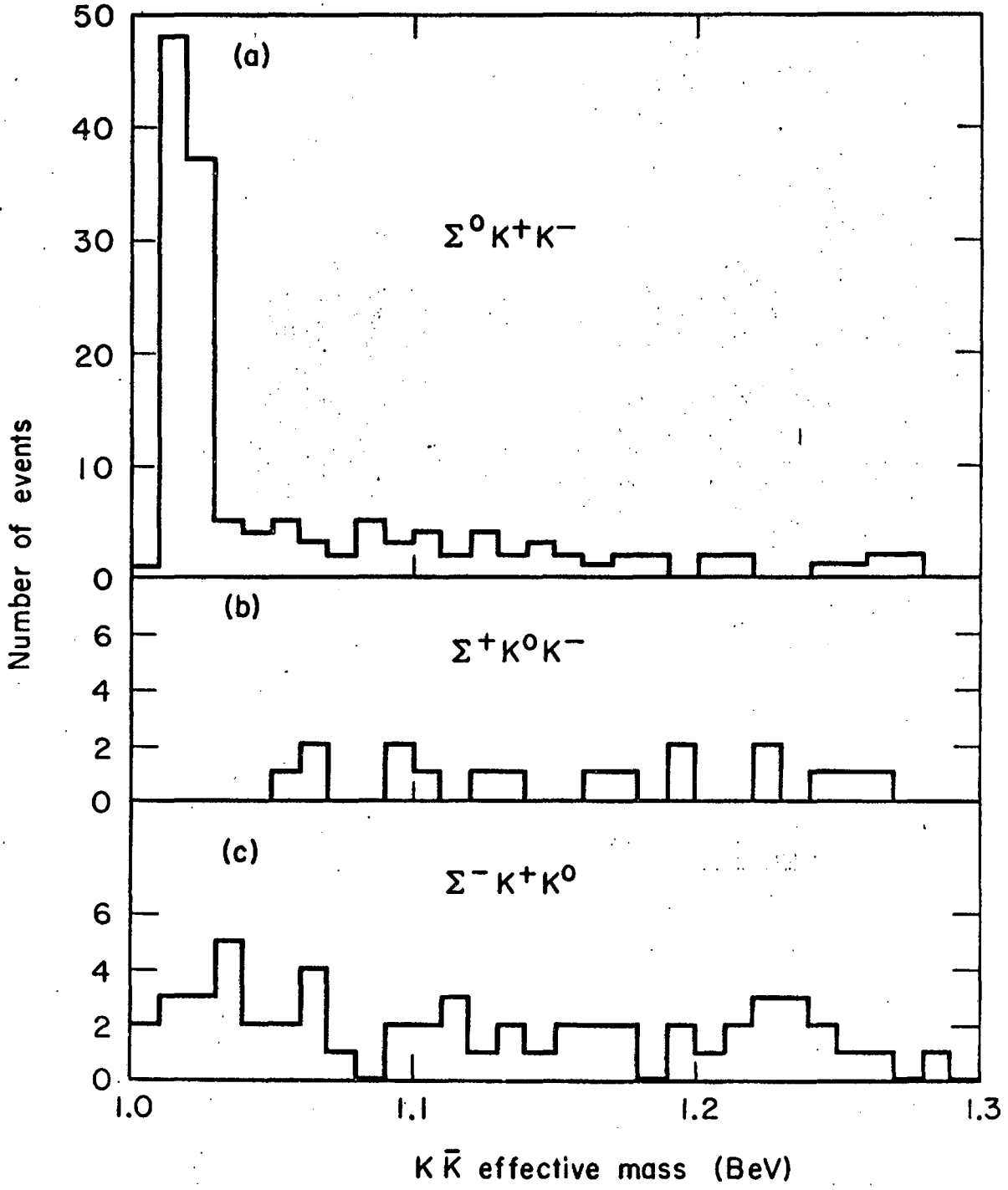

Fig. 9

MU-37116

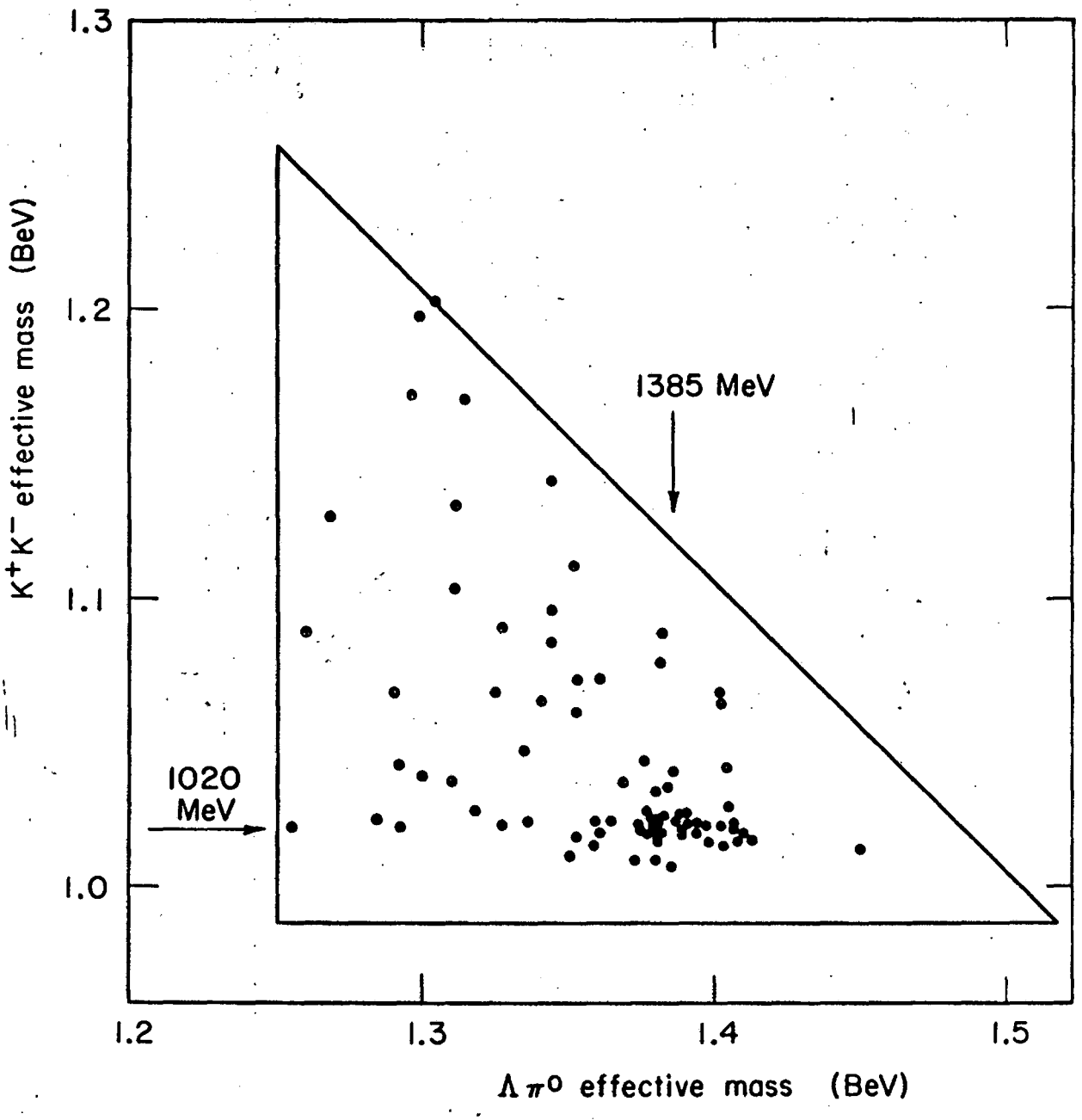
1.3
1.2
1.1
1.0
K^+K^- effective mass (BeV)
1385 MeV
1020 MeV
1.2
1.3
1.4
1.5
$\Lambda\pi^0$ effective mass (BeV)
MU-37117

Fig. 10

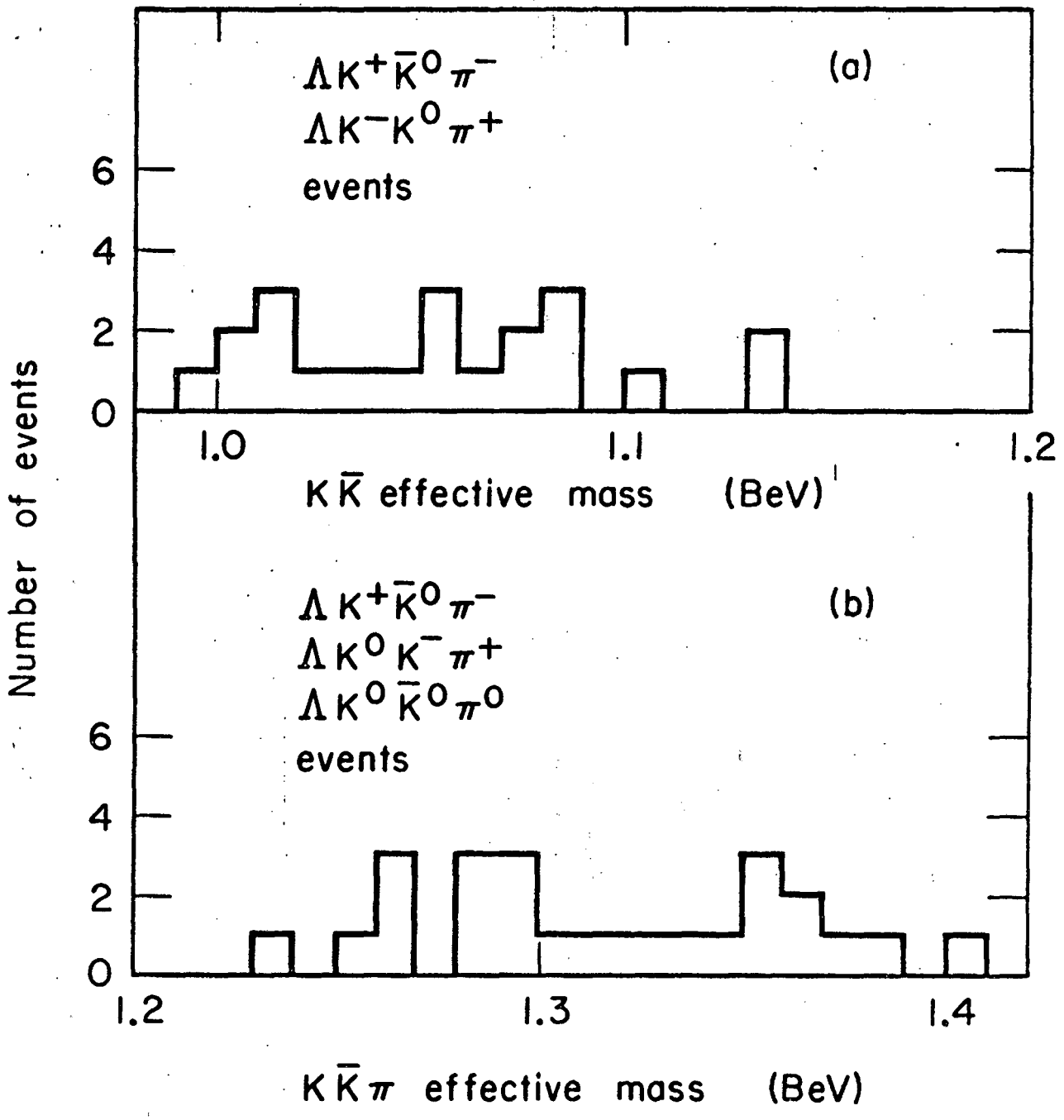

Fig. 11

MU-37118